ORIGINAL ARTICLE

Synthesis and Spectroscopic Studies of N,N'-dialkyl Derivatives of Antisymmetrical 2H,5H-Dihydropyrrolo [3,4-c]pyrrole-1,4-diones

Secil Celik Erbas · Serap Alp

Abstract 2,5-dihydropyrrolo[3,4-c]pyrrole-1,4-dione derivatives (DPP) are chemically stable, fluorescent molecules, known as High Performance Pigments. Preparation of the soluble derivatives of DPPs provides great advantage in designing the optic sensor for new and existing applications and overcoming aggregation problems in solid matrices. For this purpose, the synthesis of antisymmetric DPPs and the formation of new organic dyes through N,N'-dialkylation and their spectroscopic studies have been carried out both in solutions and in solid phase.

Introduction

Diketopyrrolopyrrole derivatives (DPPs) have been used in plastic coloring, surface coatings, and as colour filters due to their luminous colours as well as high stability. Today they are widely used in many optic systems, such as information storage and monitoring devices. In most of the recent studies, the usages of DPPs in optic systems have been taken into consideration. For example Fukuda et al., have developed a thin film ring laser system using DPP derivatives. DPPs have also been used as

S. C. Erbas · S. Alp
Department of Chemistry, University of Dokuz Eylul, The Graduate School of Natural and Applied Sciences, 35160 Izmir, Turkey

S. C. Erbas
e-mail: secil.celik@cbu.edu.tr

S. Alp (✉)
Department of Chemistry, University of Dokuz Eylul, Faculty of Sciences, 35160 Izmir, Tinaztepe, Turkey
e-mail: serap.alp@deu.edu.tr

organic semiconductors for organic solar cell applications and have been converted a 'latent' pigment [1–13].

When the literature on DPPs is scrutinized, it becomes clear that the spectroscopic characteristics of DPPs are related to the 3,6-diaryl moieties. The effect of electron-donor and electron-acceptor groups on the aryl moieties has been investigated through maximum absorption wavelengths [14].

In this study, six new antisymmetrical DPP derivatives have been synthesized by base catalyzed condensation reactions using aromatic nitriles and pyrrolinone esters. Furthermore, structural analysis, photophysical characteristics and photostabilities of the newly prepared DPPs in different media are reported.

Thus, antisymmetric 3-phenyl,6-pyridyl-2,5-dimethyl-pyrrolo[3,4-c]pyrrole-1,4-dione (DPP-1a), Diethyl-2,2'-(1,4-dioxo-3-phenyl-6-pyridine-4-yl-pyrrolo[3,4-c]pyrrole-2,5-diyl)diacetate (DPP-1b), 3-tolyl,6-pyridyl-2,5-dimethyl-pyrrolo[3,4-c]pyrrole-1,4-dione (DPP-2a), Diethyl-2,2'-[1,4-dioxo-3-(4-methylphenyl)-6-pyridine-4-yl-pyrrolo[3,4-c]pyrrole-2,5-diyl)diacetate (DPP-2b), 3-methoxyphenyl,6-phenyl-2,5-dimethylpyrrolo[3,4-c]pyrrole-1,4-dione (DPP-3a) and Diethyl-2,2'-[1,4-dioxo-3-(4-p-methoxyphenyl)-6-phenylpyrrolo[3,4-c]pyrrole-2,5-diyl)diacetate (DPP-3b) derivatives have been synthesized and their structural identifications have been made using FT-IR, NMR and LC-MS spectra. To determine the photophysical characteristics of the six newly synthesized DPPs, UV–vis absorption and emission spectroscopy techniques have been used. The maximum absorption and emission wavelengths, molar extinction coefficients (ε), singlet energy levels (Es), Stokes' shift values ($\Delta\lambda$) and quantum yields (φ_F) of DPPs are given. In addition, the photostabilities of all derivatives have been investigated in solutions of dimethylformamide (DMF), acetonitrile (ACN), chloroform (CHCl$_3$), tetrahydrofuran (THF), toluene and in a solid matrix of PVC.

Figure 1 shows schematic structures of the six different synthesized antisymmetrical N,N'-dialkyl DPP derivatives.
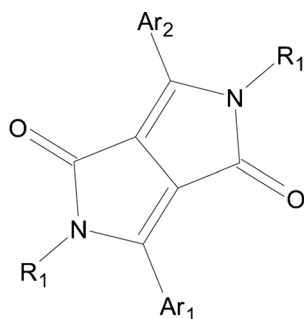
Fig. 1 Schematic structures of the antisymmetrical N,N'-dialkyl DPP derivatives (a) 3-phenyl,6-pyridyl-2,5-dimethyl-pyrrolo[3,4-c]pyrrole-1,4-dione **(DPP-1a)** [Ar₁: -phenyl, Ar₂: -pyridyl, R₁:-methyl] (b) Diethyl-2,2'-(1,4-dioxo-3-phenyl-6-pyridine-4-yl-pyrrolo[3,4-c]pyrrole-2,5-diyl)diacetate **(DPP-1b)** [Ar₁:-phenyl, Ar₂:-pyridyl, R₁:-ethylacetate] (c) 3-tolyl,6-pyridyl-2,5-dimethyl-pyrrolo[3,4-c]pyrrole-1,4-dione **(DPP-2a)** [Ar₁:-tolyl, Ar₂:-pyridyl, R₁:-methyl] (d) Diethyl-2,2'-[1,4-dioxo-3-(4-methylphenyl)-6-pyridine-4-yl-pyrrolo[3,4-c]pyrrole-2,5-diyl)diacetate **(DPP-2b)** [Ar₁:-tolyl, Ar₂:-pyridyl, R₁:-ethylacetate] (e) 3-methoxyphenyl,6-phenyl-2,5-dimethylpyrrolo[3,4-c]pyrrole-1,4-dione **(DPP-3a)** [Ar₁:methoxyphenyl, Ar₂:phenyl, R₁:-methyl] (f) Diethyl-2,2'-[1,4-dioxo-3-(4-p-methoxyphenyl)-6-phenylpyrrolo[3,4-c]pyrrole-2,5-diyl)diacetate **(DPP-3b)** [Ar₁: methoxyphenyl, Ar₂:phenyl, R₁:-ethylacetate]

Results and Discussion

Absorption and Emission Based Studies

The photophysical properties of the DPP derivatives were characterized in dimethylformamide (DMF), acetonitrile (ACN), chloroform (CHCl₃), tetrahydrofuran (THF) and toluene solvents and in the solid matrix of PVC by means of UV–vis absorption and emission spectroscopy.

Data related with UV–vis spectroscopy; maximum absorption wavelengths (λ_{max}; in nm), molar extinction coefficients (ε; in $L\,mol^{-1}\,cm^{-1}$), singlet energy levels (E_s, kj/mol) of the DPP derivatives for all the solvents used are shown in Tables 1, 2, 3, 4, 5 and 6 respectively. Quantum yield values were calculated in THF only because it was found to be an appropriate solvent which has the same characteristics with the standard used.

The DPP derivatives (DPP-1a, 1b, 2a, 2b, 3a, 3b) exhibited maximum absorption wavelengths between 460–473 nm, 458–467 nm, 470–493 nm, 462–483 nm, 476–485 nm and 466–468 nm respectively in all of the solvents and they showed maximum absorption wavelengths between 472–495 nm in the solid matrix of PVC. When all of the absorption spectrum of the DPP derivatives are analyzed, a bathochromic shift is observed in toluene relative to the other solvents (see Fig. 2). This shift can be attributed to the π-π interactions between the aromatic rings of the DPP derivatives and toluene. The bathochromic shifts of the absorption wavelength of the studied DPP derivatives in the PVC matrix are generally higher than in solvents media. This can be attributed to the decreasing of the molecular mobility and increasing of the conjugation. Only the DPP-2b derivative showed a hypsochromic shift. The ethyl acetate groups which are attached to the nitrogen atoms in DPP-2b, can not be found in the same plane with the phenyl rings at the 3 and 6 positions of the DPP core [15, 16].

The molar absorption coefficient values of all DPPs were found to be quite enough for different applications. Especially in PVC matrix, this value was found to be the highest one which can be attributed to the rigidity of the immobilized phase.

The emission spectroscopic data of the fluorescent DPP derivatives are shown in Tables 1, 2, 3, 4, 5 and 6.

DPP-1a, 1b, 2a, 2b, 3a, 3b exhibited maximum emission wavelengths between 528–532 nm, 523–529 nm, 542–

Table 2 UV–vis spectroscopic data (λ/nm, ε/$Lmol^{-1}\,cm^{-1}$) and emission spectroscopic data (E_s, kcal/mol; φF) of DPP-1b

Solvent	$\lambda_{abs.}$ (nm)	$\lambda_{ex.}$ (nm)	λ^f_{max} (nm)	ε $Lmol^{-1}\,cm^{-1}$	$\Delta\lambda$	E_S kcal/mol	φF
DMF	464	463	526	9,500	62	62	
ACN	458	455	523	20,000	65	62	
CHCl₃	464	464	525	15,333	61	62	
THF	466	465	525	20,000	59	61	0,83
Toluen	467	466	529	20,000	62	61	
PVC	472	461	525	172,413	53	61	

Table 1 UV–vis spectroscopic data (λ/nm, ε/$Lmol^{-1}\,cm^{-1}$) and emission spectroscopic data (E_s, kcal/mol; φF) of DPP-1a

Solvent	$\lambda_{abs.}$ (nm)	$\lambda_{ex.}$ (nm)	λ^f_{max} (nm)	ε $Lmol^{-1}\,cm^{-1}$	$\Delta\lambda$	E_S kcal/mol	φF
DMF	467	467	530	13,667	63	61	
ACN	460	460	528	14,000	68	62	
CHCl₃	468	468	530	13,667	62	61	
THF	468	466	529	14,333	61	61	0,76
Toluen	473	469	532	5,167	59	60	
PVC	477	473	528	37,140	51	60	

Table 3 UV–vis spectroscopic data (λ/nm, ε/$Lmol^{-1}\,cm^{-1}$) and emission spectroscopic data (E_s, kcal/mol; φF) of DPP-2a

Solvent	$\lambda_{abs.}$ (nm)	$\lambda_{ex.}$ (nm)	λ^f_{max} (nm)	ε $Lmol^{-1}\,cm^{-1}$	$\Delta\lambda$	E_S kcal/mol	φF
DMF	470	483	548	5,667	78	61	
ACN	477	475	538	6,667	61	61	
CHCl₃	474	484	545	6,667	71	60	
THF	470	484	542	4,167	72	61	0,73
Toluen	493	482	542	18,000	49	58	
PVC	491	477	544	32,787	53	58	

Table 4 UV–vis spectroscopic data (λ/nm, ε/Lmol^{-1} cm^{-1}) and emission spectroscopic data (E_s, kcal/mol; φF) of DPP-2b

Solvent	$\lambda_{abs.}$ (nm)	$\lambda_{ex.}$ (nm)	λ^f_{max} (nm)	ε Lmol^{-1} cm^{-1}	$\Delta\lambda$	E_S kcal/mol	φF
DMF	469	468	530	13,000	61	61	
ACN	462	462	528	35,000	66	62	
CHCl$_3$	470	466	530	33,333	60	61	
THF	469	467	530	40,000	61	61	0,79
Toluen	483	467	533	23,333	50	59	
PVC	480	466	529	50,000	49	59	

Table 6 UV–vis spectroscopic data (λ/nm, ε/Lmol^{-1} cm^{-1}) and emission spectroscopic data (E_s, kcal/mol; φF) of DPP-3b

Solvent	$\lambda_{abs.}$ (nm)	$\lambda_{ex.}$ (nm)	λ^f_{max} (nm)	ε Lmol^{-1} cm^{-1}	$\Delta\lambda$	E_S kcal/mol	φF
DMF	467	472	521	10,000	54	61	
ACN	462	460	518	3,667	56	62	
CHCl$_3$	466	466	522	14,333	56	61	
THF	466	466	520	14,167	54	61	0,99
Toluen	468	473	523	29,000	50	61	
PVC	473	466	525	37,941	52	60	

548 nm, 528–533 nm, 525–531 nm and 520–523 nm respectively in all of the solvents used and significant bathofluoric shifts in the maximum emission wavelenghts were observed in toluen relative to the other solvents (see Fig. 3). In PVC matrices, maximum emission wavelengths are between 525–544 nm as in toluene. In a similar way, the DPP core which has phenyl rings at the 3 and 6 positions exhibited a bathofluoric shift but the other aromatic moieties didn't show any significiant shift. This result can be attributed to the difference between the HOMO-LUMO energy levels of different aryl groups.

The singlet energy levels (E_s) of these derivatives were estimated to be about 58–62 kcal/mol. These values are smaller in the PVC matrix with respect to the studied solvents.

The Stokes' shift values are in the range 44–78 nm in solutions. When doped into PVC, this value is between 37 and 53 nm. A large Stokes' shift is often highly desirable for fluorescence measurements in sensor studies.

Photostability Studies

The photostabilities of the DPP derivatives were measured in DMF, ACN, CHCl$_3$, THF, toluene and PVC (see Fig. 4). Photostability tests of DPP derivatives were performed by using a steady state spectrofluorimeter in the mode of "Time Based Measurements" employing a xenon arc lamp. All of the fluorophores were excited at around 470 nm and the data were

obtained at their maximum emission wavelengths for one hour of monitoring. The acquired data of DPP-2b is shown in Fig. 4. These results are compatible with 3,6-diphenyl-2,5-dihexyl-1,4-diketopyrrolo[3,4-c]pyrrole-1,4-dione's photostability results (see Fig. 5) which has been published before [17].

Fluorescence Quantum Yield Calculations

Fluorescence Quantum Yield values (φF) of the DPP derivatives were measured using the comparative William's method [18], which involves the use of standards with known φF values. For this purpose, the UV–vis absorbance and corrected emission spectra of five different concentrations of DPP derivatives and reference standards (Perylenediimide N, N-didodecyl λex=470 nm) were recorded. The integrated fluorescence intensities of the DPP dyes were plotted as a function of absorbance values. The quantum yield of the studied molecules was proportional to the gradients of the plots. To protect from the inner filter effect; the optical densities of the standards and unknown were kept constant at less than 0.1 at the excitation wavelength. Unknown and standard solutions which were used in the measurement of quantum yields have the same optical density. For this reason, the actual quantum efficiencies of the standards and samples were compared. The formula is applied to correct the differences arising from the

Table 5 UV–vis spectroscopic data (λ/nm, ε/Lmol^{-1} cm^{-1}) and emission spectroscopic data (E_s, kcal/mol; φF) of DPP-3a

Solvent	$\lambda_{abs.}$ (nm)	$\lambda_{ex.}$ (nm)	λ^f_{max} (nm)	ε Lmol^{-1} cm^{-1}	$\Delta\lambda$	E_S kcal/mol	φF
DMF	481	476	529	11,833	48	59	
ACN	476	470	525	9,333	49	60	
CHCl$_3$	481	476	528	9,000	47	59	
THF	484	477	528	9,000	44	59	0,96
Toluen	485	479	531	7,833	46	59	
PVC	495	482	532	128,000	37	58	
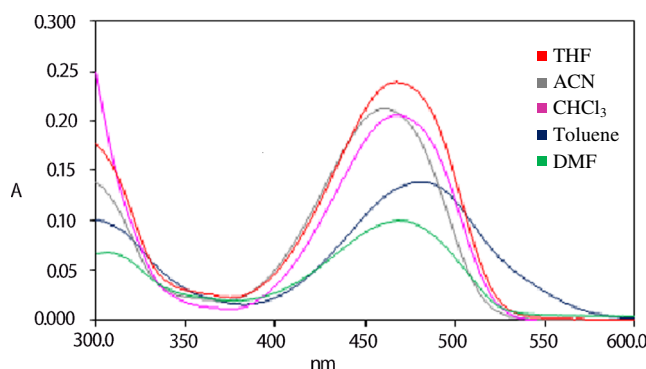
Fig. 2 Absorption spectrum of DPP-2b in different solvents
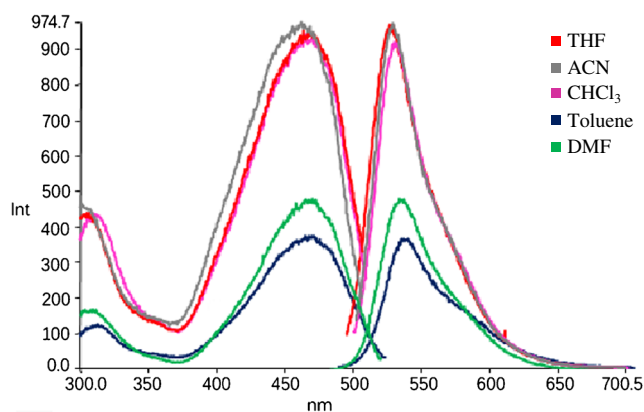
Fig. 3 Emission and excitation spectrum of DPP-2b in different solvents
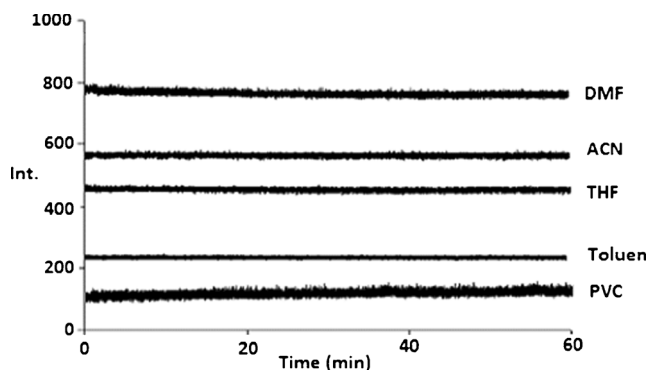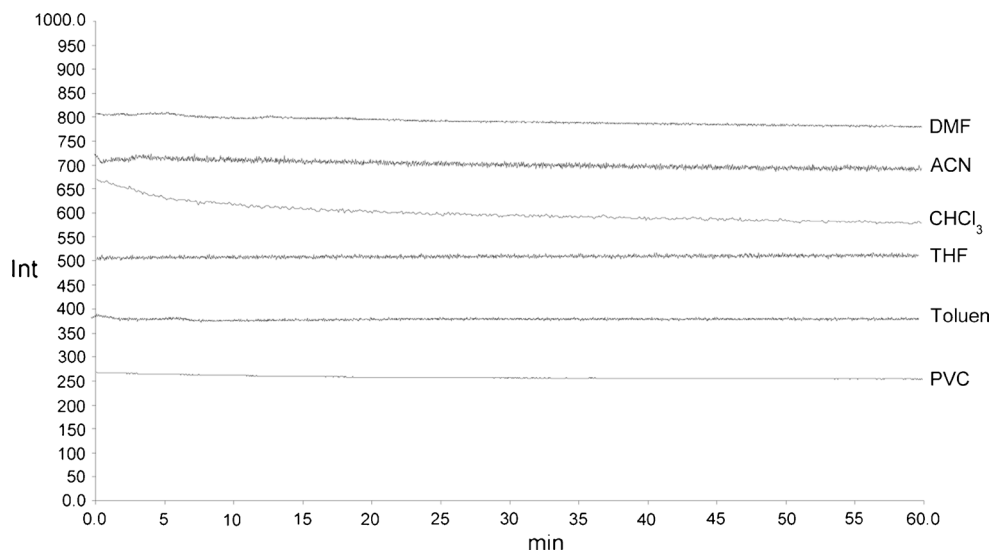

Fig. 5 Photostability results of 3,6-diphenyl-2,5-dihexyl-1,4-diketopyrrolo[3,4-c]pyrrole-1,4-dione in all studied solvents [17]

refractive index of the matrices. Quantum yield (φF) values were evaluated according to the following equation where ST and X denote standard and sample respectively, Grad is the gradient from the plot and n is the refractive index of the solvent [19].

$$\Phi_{Sample} = \Phi_{ST} \left(Grad_x / Grad_{ST} \right) \left(\eta_x^2 / \eta_{ST}^2 \right)$$

The quantum yield value of DPP-3 is higher than DPP-1 and DPP-2. This increase can be attributed to the rich electron donation of the methoxy group which is connected to the phenyl ring.

Experimental

Instrumental

A Bamstead Electrothermal 9,100 apparatus was used for determining melting points. KBr pellets of three derivatives were prepared and used on a Perkin-Elmer Spectrum BX FTIR spectrometer for IR spectra. NMR spectra were recorded on a Unity Inova 500 (Varian) Instrument and chemical shifts are expressed in ppm downfield from $SiMe_4$. An Agilent 1260 Infinity Liquid Chromatography- Agilent 6420 Triple Quadrupole Mass Spectrometry was used for mass spectra. A Shimadzu 1601 UV-Visible spectrophotometer was used for absorption spectra. A Varian Cary Eclipse Spectrofluorimeter with a Xenon flash lamp as the light source was used to measure steady state fluorescence emission and excitation spectra.

All the experiments were carried out at room temperature; 25±1 °C. Perylenediimide N,N-didodecyl was used as a reference standard for fluorescence quantum yield calculations of the DPP.

Reagents

All reagents were obtained from Merck and Fluka. Chromatographic grade solvents were used in chromatographic separation and crystallization processes. Solvents used in spectroscopic
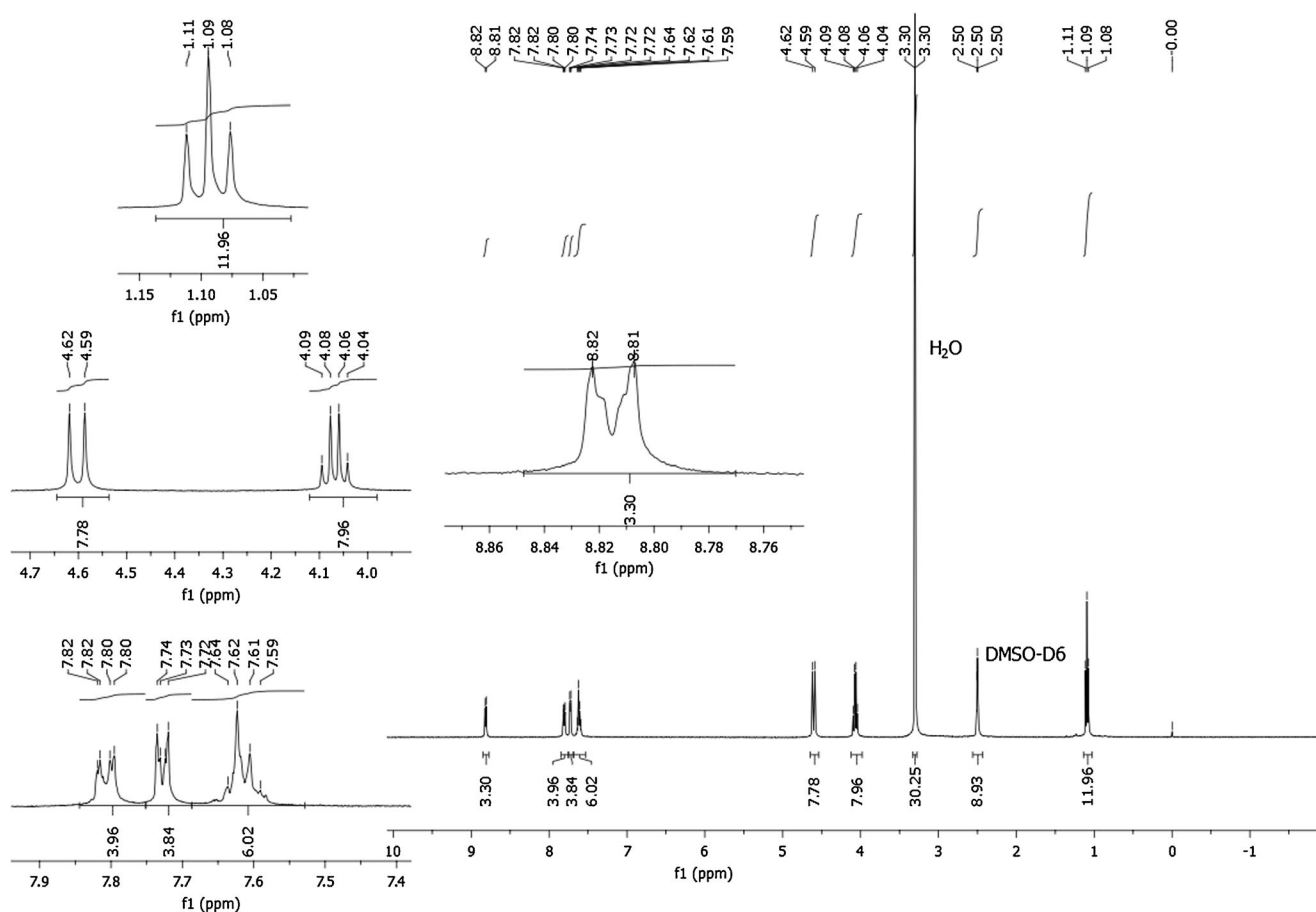
Fig. 4 Photostability results of DPP-2b in all studied solvents and solid matrix (PVC)

Fig. 6 The ^{1}H-NMR spectrum of the DPP-1b

studies were of analytical grade and used without a purification process.

Synthesis

The intermediate product pyrrolinone ester derivatives were prepared in three steps by following the literature procedure[20].

DPP derivatives were synthesized by base catalyzed condensation of equivalent numbers of an aromatic nitrile e.g. 4-pyridiylcarbonitrile, p-methoxybenzonitrile with a pyrrolinone ester i.e. ethyl-4,5-dihydro-5-oxo-2-phenyl(1H)-pyrrole-3-carboxylate, ethyl-4,5-dihydro-5-oxo-2-tolyl(1H)-pyrrole-3-carboxylate [21].

Alkylation of DPP derivatives was carried out in the presence of sodium hydride as a base in 1-methyl-2-pyrrolidone. Ethylbromoacetate and dimethylsulphate were used as alkylating agents.

2-(4-arylbenzoyl)Acetic Acid Ethyl Ester

The procedure used for the synthesis of 2-(4-arylbenzoyl)acetic acid ethyl ester:

A suspension of sodium hydride (60 % suspension in paraffine oil, 330 mmol) in diethyl carbonate was heated to 100 °C. During 4 h, acetophenone derivative (acetophenone, 4'-methyl acetophenone) (300 mmol) dissolved in diethyl carbonate was added under vigorous stirring. Stirring was continued for 30 min at the same temperature, then the solution was allowed to cool to r.t. After adding water and acetic acid, the solution was stirred overnight. The aqueous phase was extracted twice with diethyleter. The combined organic layers were washed with saturated aqueous solutions of NaHCO$_3$ and NaCl. After drying (MgSO$_4$), the solvent was evaporated under reduced pressure. The residue was used for the next step without further purification.

2-(4-arylbenzoyl)Maleic Acid Diethyl Ester

The procedure used for the synthesis of 2-(4-arylbenzoyl)maleic acid diethyl ester:

A mixture of 2-(4-arylbenzoyl)acetic acid ethyl ester (44 mmol), ethyl-2-bromoacetate (53 mmol) and potassium carbonate (51 mmol) in acetone was heated under reflux for 20 h. After cooling to r.t., the suspension was filtered and the salts were washed with diethylether. The organic layers were

Table 7 Structural analyses values of DPP derivatives

DPP-1a	as red-orange crystal (yield; 3.6 %) **mp** 148,7–149,5 °C. **FT-IR [KBr, $\tilde{\nu}$ max (cm^{-1})]:** 3036 (=CH$_{stretch}$), 2851-2921 (C-H$_{stretch}$), 1684 (lactam C=O$_{stretch}$). **^{1}H-NMR [DMSO-d$_6$, δ_H (ppm)]:** 2.480 s (6H), 7.400 d (2H), 7.700 m (5H), 8.800 d (2H). **LC-MS:** MW=317 Da; m/z 318 (M+H)
DPP-1b	as red-crystal (yield; 10 %) **mp** 133,3–133,5 °C. **FT-IR [KBr, $\tilde{\nu}$ max (cm^{-1})]:** 3047–3075 (=CH$_{stretch}$), 2923–2985 (C-H$_{stretch}$), 1739 (ester C=O$_{stretch}$), 1662 (lactam C=O$_{stretch}$). **^{1}H-NMR [DMSO-d$_6$, δ_H (ppm)]:** 1.095 t (6H), 4.069 q (4H), 4.587 s (2H), 4.619 s (2H), 7.606–7.624 d, dd (3H), 7.722–7.737 d (2H), 7.797–7.819 dd (2H), 8.808–8.823 d (2H). **LC-MS:** MW=461 Da; m/z 462 (M+H)
DPP-2a	as red-orange crystal (yield; 35 %) **mp** 255–257 °C. **FT-IR [KBr, $\tilde{\nu}$ max (cm^{-1})]:** 3035 (=CH$_{stretch}$), 2924–2952 (C-H$_{stretch}$), 1673 (lactam C=O$_{stretch}$). **^{1}H-NMR [CDCl$_3$, δ_H (ppm)]:** 2.450 s (3H), 3.350 s (6H), 7.360 d (2H), 7.760 d (2H), 7.830 d (2H), 8.810 d (2H). **LC-MS:** MW=331 Da; m/z 332 (M+H)
DPP-2b	as orange-crystal (yield; 26 %) **mp** 118–120 °C. **FT-IR [KBr, $\tilde{\nu}$ max (cm^{-1})]:** 3030 (=CH$_{stretch}$), 2929–2989 (C-H$_{stretch}$), 1732 (ester C=O$_{stretch}$), 1683 (lactam C=O$_{stretch}$). **^{1}H-NMR [DMSO-d$_6$, δ_H (ppm)]:** 1.087 t (3H), 1.075 t (3H), 2.393 s (3H), 4.047 q (2H), 4.059 q (2H), 4.564 s (2H), 4.596 s (2H), 7.391–7.412 d (2H), 7.691–7.715 d, d (4H), 8.800 d (2H). **LC-MS:** MW=475 Da; m/z 476 (M+H)
DPP-3a	as red-orange crystal (yield; 40 %) **mp** 184–185 °C. **FT-IR [KBr, $\tilde{\nu}$ max (cm^{-1})]:** 3053 (=CH$_{stretch}$), 2952–2985 (C-H$_{stretch}$), 1680 (lactam C=O$_{stretch}$). **^{1}H-NMR [DMSO-d$_6$, δ_H (ppm)]:** 3.240–3.260 s (6H), 3.880 s (3H), 7.150 d (2H), 7.585 d (3H), 7.925 d (2H), 7.990 d (2H). **LC-MS:** MW=346 Da; m/z 347 (M+H)
DPP-3b	as orange-yellow crystal (yield; 55 %) **mp** 168–170 °C. **FT-IR [KBr, $\tilde{\nu}$ max (cm^{-1})]:** 3072 (=CH$_{stretch}$), 2939–2971 (C-H$_{stretch}$), 1739 (ester C=O$_{stretch}$), 1680 (lactam C=O$_{stretch}$). **^{1}H-NMR [CDCl$_3$, δ_H (ppm)]:** 1.200 t (6H), 3.870 s (3H), 4.190 q (4H), 4.500 s (4H), 7.000 d (2H), 7.500 dd (3H), 7.770 d (4H). **^{13}C NMR (DMSO-d6, ppm):** 14.53; 14.56; 43.88; 44.07; 56.28; 61.98 (2xC); 108.08; 109.17; 115.30 (2xC); 119.94; 127.85; 129.11(2xC); 129.72 (2xC); 131.31(2xC); 132.13; 147.27; 148.95; 161.90; 162.21; 162.65; 169.09; 169.12. **LC-MS:** MW=490 Da; m/z 491 (M+H)

combined, the solvent was evaporated off under reduced pressure, and the residue was used for the next step without further purification.

2-(4-aryl)-3-ethoxycarbonyl-2-pyrroline-5-on

The procedure used for the synthesis of 2-(4-aryl)-3-ethoxycarbonyl-2-pyrroline-5-on:

Ammonium acetate (600 mmol) and 2-(4-aryl)-3-ethoxycarbonyl-2-pyrroline-5-on (55 mmol) were refluxed in acetic acid for 3 h (oil-bath temperature: 125 °C). After cooling to r.t., ice water was added to the dark green solution with rapid stirring. The residue was filtered, dried under vacuum and re-crystallization was performed from methanol for all derivatives.

3-phenyl-6-pyridine-2,5-dihydropyrrolo [3,4-c]pyrrole-1,4-dione and 3-tolyl-6-pyridine-2,5-dihydropyrrolo [3,4-c]pyrrole-1,4-dione

The procedure used for the synthesis of 3-tolyl-6-pyridine-2,5-dihydropyrrolo[3,4-c]pyrrole-1,4-dione:

Pyridine-4-carbonitrile (20 mmol) was added, under stirring and a nitrogen atmosphere, to a solution of sodium t-amyl oxide [from sodium metal (60 mmol)] in dry t-amyl alcohol. Natrium was dissolved under reflux in the catalytic presence of FeCl$_3$ (it takes approximately 2 h). 2-(4-phenyl)-3-etoxycarbonyl-2-pyrroline-5-on and 2-(4-tolyl)-3-ethoxycarbonyl-2-pyrroline-5-on (10 mmol) was added

portionwise at 100 °C above 30 s. The mixture was stirred for 1 h at 100 °C and 24 h at r.t. Finally, the mixture was poured into cold water. T-amyl alcohol was evaporated and the residue was filtered off, washed with methanol and dried under vacuum.

3-phenyl-6-methoxyphenyl-2, 5-dihydropyrrolo[3,4-c]pyrrole-1,4-dione

This derivative was prepared by the same procedure using the appropriate starting materials.

N,N'-dialkylation of DPP

The procedure used for synthesis of N,N'-dialkyl derivatives of antisymmetric DPPs:

DPP derivative was stirred in 1-methyl-2-pyrrolidone at room temperature. Sodium hydride was added under a nitrogen atmosphere. After that, n-alkyl halide (dimethylsulphate, ethylbromo acetate) was added and stirred for 18 h. The mixture was poured into water. The precipitate was filtered off and the crude product was re-crystallized from methanol for all derivatives.

Structural Analysis

The NMR spectra of the DPP-1b were indicated in Fig. 6. All structural analysis results are reported in Table 7.

References

1. Wallquist O, Lenz R (2002) Twenty years of DPP pigments-future perspectives. Macromol Symp 187:617–629

2. Hao Z, Iqbal A (1997) Some aspects of organic pigments. Chem Soc Rev 26:203–213

3. Wallquist O (2002) Diketopyrrolopyrrole (DPP) pigments. Wiley-VCH publishers, Verlag GmbH & Co. In High Performance Pigments

4. Maloney J (2002) In: Smith H (ed) Titanate pigments: Colored rutile, priderite and pseudo-brookite structured pigments. Wiley-VCH, Weinheim, pp 159–184

5. Zambounis JS, Hao Z, Iqbal A (1997) Latent pigments activated by heat. Nature (London) 388:131–132

6. Rochat AC, Wallquist O, Iqbal A, Mizuguchi J (1999) Process for the preparation of aminated diketobis (aryl or heteroaryl)pyrrolopyrroles and the use thereof as photoconductive substances. US Patent 5,973,146

7. Fukuda M, Kodama K, Yamamoto H, Mito K (2002) Solid-state laser with newly synthesized pigment. Dyes Pigments 53:67–72

8. Fukuda M, Kodama K, Yamamoto H, Mito K (2004) Evaluation of new organic pigments as laser-active media for a solid-state dye laser. Dyes Pigments 63:115–125

9. Langhals H (1990) Erasable optical fluorescence and absorption data medium having good long-term stability. Ger Pat DE 3901988

10. Mizuguchi J, Rochat CA (1988) A new near-infrared photoreceptor based on 1,4-dithioketo-3,6-diphenyl-Pyrrolo-[3,4-c]-pyrrole. J Imaging Sci 32:135–140

11. Vala M, Vyňuchal J, Toman P, Weiter M, Luňák S Jr (2010) Novel, soluble diphenyl-diketo-pyrrolopyrroles: experimental and theoretical study. Dyes Pigments 84:176–182

12. Prashant S, Ng G, Lin T, Dodabalapur A, Chen Z (2010) Solution processable low bandgap diketopyrrolopyrrole (DPP) based derivatives: novel acceptors for organic solar cells. J Mater Chem 20:3626–3636

13. Horn M (1999) Flüssigkristalline pyrrolopyrrol-derivative. Blunk-Verlag, Berlin

14. Luňák S, Vyňuchal J, Vala M, Havel L, Hrdina R (2009) The synthesis, absorption and fluorescence of polar diketo-pyrrolopyrroles. Dyes Pigments 82:102–108

15. Vala M, Weiter M, Vynuchal J, Toman P, Lunak S (2008) Comparative studies of diphenyl-diketo-pyrrolopyrrole derivatives for electroluminescence applications. J Fluoresc 18:1181–1186

16. Weiter M, Salyk O, Bednar P, Vala M, Navratil J, Zmeskal O, Vynuchal J, Lunak S (2009) Morphology and properties of thin films of diketopyrrolopyrrole derivatives. Mater Sci Eng B 165:148–152

17. Celik S, Ergun Y, Alp S (2009) Synthesis and spectroscopic studies of 3,6-diphenyl-2,5-dihydropyrrolo[3,4-c]pyrrole-1,4-dion's N, N'-dialkyl derivatives. J Fluoresc 19:829–835

18. Williams ATR, Winfield SA, Miller JN (1983) Relative fluorescence quantum yields using a computer-controlled luminescence spectrometer. Analyst 108:1067–1071

19. Valeur B (2002) Molecular fluorescence: Principles and applications. Wiley-VCH Verlag GmbH, Weinheim

20. Horn M, Hepuzer Y, Yagci Y, Bilgin-Eran B, Cernenco U, Harabagiu V, Pinteala M, Simionescu CB (2002) Synthesis and characterisation of thermomesogenic polysiloxanes with 2,5-dihydropyrrolo[3,4-c]pyrrole-1,4-dione units in the main chain. Eur Polymer J 38:2197–2205

21. Pfenninger J, Iqbal A, Rochat AC (1988) Process for the preparation of pyrrolo[3,4-c]pyrroles. United States Pat. 4.749.795